ADAPTIVE-WALL TECHNOLOGY APPLIED TO THE DERA 8FT HIGH SPEED WIND TUNNEL (HST)

N J Taylor, Matra BAe Dynamics Ltd., P R Ashill, Cranfield University, M J Simmons, DERA
nigel-j.taylor@bae.co.uk
Keywords: *Adaptive walls, wind tunnel, wall-interference corrections*

Abstract

Research aimed at extending the subsonic Mach-number range of the 8ft High Speed wind Tunnel (HST) at the Defence Evaluation and Research Agency (DERA) Bedford to values in excess of 0.9 is described. This has been achieved by adapting the flexible roof and floor liners of the test section, normally used to provide supersonic flows. To test the effectiveness of the wall adaptation, two models have been tested with different wall shapes; these were a half model of a combat aircraft wing body and a generic research model to study transport wing-body configurations. It was found that wall adaptation was able to extend the range of Mach numbers at which both half and complete models could be tested from 0.87 to about 0.95. The standard method for correcting Mach number, which uses wall pressure measurements, was shown to provide for virtually all the effects of wall interference. The small additional effects are readily allowed for by a simple method described in the paper.

Symbols

B	breadth of test section
C_D	drag coefficient
C_L	lift coefficient
C_m	pitching moment coefficient
C_p	static pressure coefficient
ETA	non-dimensional spanwise position
H	reference total pressure
M_c	corrrected Mach number
M_R	reference Mach number
p	static pressure
R	Reynolds number based in aerodynamic mean chord
u	increment in streamwise velocity
u_w	the mean of the measured streamwise velocity increments at corresponding points on the roof and floor of the test section due to the presence of the model
x	streamwise station (defined positive upstream of the tunnel reference in tunnel axes and positive downstream of the wing leading edge in model axes)
y	wall displacement, defined positive away from the tunnel centre-line
α	angle of incidence
δu_B	additional correction to blockage increment in streamwise velocity due to wall shaping and the effect of the wall boundary layers on the factor λ
λ	blockage factor
Δ	increment due to the change from straight to contoured walls

Suffixes

B	blockage
bl	due to the effect of the boundary layers on the ratio λ
fw	due to the change from straight to flexible wall shape
i	inviscid flow

1 Introduction

Closed wind tunnels are rarely used for testing at Mach numbers in the range 0.9 to 1.4. This arises primarily because of the gross interference effect of the walls on the flow around the model in this region. Thus, for example, the correction to Mach number to allow for this interference rises rapidly as the test Mach number approaches unity, resulting in the phenomenon of choking. This represents a severe limitation and, in the late 1940's, prompted the development of the ventilated-wall working section [1].

While ventilated-wall wind tunnels allow tests to be performed for Mach numbers around unity, they have one disadvantage over solid wall tunnels. This is that the wall boundary conditions are not well understood. Consequently, while the

corrections for wall interference are likely to be small, they cannot be calculated using the classical potential-flow approach with the same accuracy as for solid-wall tunnels.

Before the development of ventilated-wall working sections, a number of alternative methods for extending the Mach-number range of solid-wall tunnels were studied. One of the most promising of these was developed during the 1930's at the National Physical Laboratory, Teddington, England [2]. This approach aimed to reduce the wall interference by shaping the walls of the working section. This was done manually and thus the time to take data was increased. Following the development of the ventilated-wall working section, this work came to a halt and lay dormant until, with the arrival of the high-speed digital computer during the 1960's, the idea of adapting the wall shape 'on-line' became a practical possibility. A large amount of research was undertaken in small-scale facilities at a number of research establishments [3], [4]. However, until recently, adaptive-wall technology has rarely been applied to large-scale, industrial wind tunnels.

During the 1970's DERA began a research programme on wall interference using measured boundary conditions [5], [6] and took an active interest in adaptive wall technology. This included supporting research by Prof. Goodyer and his group at Southampton University [7], [8], [9]. This paper describes a programme of research initiated and led by the first author before he left DERA. The main aim of this work is to investigate wall shaping in the 8ft High Speed Tunnel (HST) at DERA to allow data to be taken that can be corrected to 'free-air' conditions for Mach numbers up to about 0.95.

After describing the wind tunnel in Section 2, including its performance with conventional wall settings, the paper describes the aircraft models used, including a wall-mounted half model and a sting mounted complete model, and the wall-shaping strategy in Section 3. Section 4 describes the procedures used to correct the data for wall interference. The results of an assessment of the wall adaptation procedure using two different aircraft models are described and discussed in Section 5 and concluding remarks are presented in Section 6.

2 The DERA HST

The 8ft HST is a continuous-flow facility with a conventional, closed-return circuit design, permitting Mach numbers ranging from 0.13 to 0.87 and 1.4 to 2.5 to be generated in the test section, when empty. The circuit may be pressurised and the stagnation pressure varied between 0.1 and 4 atmospheres, absolute, allowing the test Mach number and Reynolds number to be varied independently. Further details of the facility and of plant dedicated to controlling its operation are provided in References 10 to 14.

The test section, illustrated in Fig 1, is 2.44m (8ft) square and 8m long, with solid parallel sidewalls and impervious flexible top and bottom walls. In supersonic operating mode, the flexible walls are used to form a variable convergent-divergent nozzle. When operating at subsonic speeds, the walls downstream of the throat are normally set to fixed divergent contours, designed to minimise the streamwise pressure gradient by accommodating the growth of the (undisturbed) wall boundary layers. In this configuration, referred to as the Mach 1 liner, the walls are effectively straight. In undertaking this programme of research it was appreciated that the flexibility of the top and bottom walls, with their associated jacks, could be used to extend the subsonic Mach number range.

The Mach number is controlled by adjusting the drive power and/or the geometry of the supersonic diffuser (not shown in Fig 1), which is used as a second throat when testing at Mach numbers above 0.5. The maximum subsonic Mach number that can be generated in this way, 0.87, is limited by the operating characteristics of the 2-stage, axial compressor used to drive the tunnel at subsonic speeds rather than any problems associated with wall interference. In fact, with the application of corrections for wall interference, it is often possible to obtain high quality test data at Mach numbers up to about 0.9, depending on the model size, attitude and, to a lesser extent, variations in ambient conditions. Nevertheless, a number of reasons were considered to justify extending the range of subsonic Mach numbers in the tunnel.

1. Planned long-range civil transport will need to have their performance characteristics demonstrated for Mach numbers up to at least 0.95.
2. Combat aircraft sustained manoeuvre performance should be studied for subsonic Mach numbers above 0.9.

3. While the magnitude of the primary correction to Mach number may make it possible to test such models at Mach numbers of about 0.9 with conventional straight walls, the residual variations of wall-induced velocities may mean that it is not possible to correct the data to 'free-air' conditions.

3 Wall shaping and experimental details

3.1 The models

The half model of a combat aircraft configuration was intended originally for research into flows over the wing at high subsonic speeds over a wide range of Reynolds numbers. With the liners set to the Mach 1 configuration, the solid-blockage ratio of this model was 0.62%. The wing was of low aspect ratio, with a semi-span of 0.821m and the model length was 2.357m. The body had a base of area 0.0188m^2. The model was mounted on the starboard sidewall at the station shown in Fig 1. The tests on this model were performed at a Reynolds number based on aerodynamic mean chord R = 14.3 x 10^6.

The solid blockage ratio of the generic transport aircraft complete model was 0.32%, the wing span being 1.58m and the length 1.28m. This model was mounted on a central sting and was located close to the position shown for sting-mounted models in Fig 1. For this model the tests were performed at R = 3.5 x 10^6.

3.2 Wall shaping

While the walls were not originally designed to be profiled to reduce wall interference, Fig 1 shows that the potential exists, especially for testing half-models, which are mounted further upstream of the ends of the flexible walls than full-models. There were, however, two significant limitations imposed by the relatively coarse spacing of the jacks at 2ft (0.61m) intervals and a minimum permissible local radius of curvature of 124ft (37.8m). It was anticipated, therefore, that the control of wall interference would not be as refined as had previously been demonstrated in smaller, purpose-built, research facilities [3], [4]. Despite these limitations, it was anticipated that significant improvements could be made to the tunnel's operating envelope without making any substantial modifications to the existing hardware.

In order to increase the maximum subsonic Mach number within the limitations of the compressor, the flexible walls were moved bodily inwards. Based on previous studies in small-scale adaptive wind tunnels [7] and in the 8ft Tunnel [15] it was argued that any streamwise variations of blockage could be minimised by profiling the walls in single curvature.

The wall shapes relative to the 'straight' or Mach 1 liners are shown in Figs 2a & b. These show y/B, the outward movement of each wall, made non-dimensional by working section breadth, B, plotted against x/B the non-dimensional axial distance upstream of the wind-tunnel reference. This reference position is close to the centre of rotation of sting-mounted complete models (Fig 1). The wall contours used for the half-model tests are illustrated in Fig 2a. The contour obtained by bodily moving the walls inwards is referred to as 'A', and the Contours B and C are attempts to relieve the locally high values of blockage. The figure also shows the wall displacement needed to compensate completely for the model volume, referred to as 'solid blockage'. Fig 2b shows the contours D and E used for the tests on the complete model. As with Contour A, these were obtained by a bodily inward movement of the walls, although the magnitude of the movements was smaller than that for A to minimise the effects on the model of wall-induced pressure gradients. The main attraction of these contours was in allowing the Mach-number range of the tunnel to be extended for complete-model testing. On the other hand, limitations imposed on wall curvature at the downstream end of the flexible liners, meant that it was not possible to provide any subtle relief for model volume effects for the complete model.
It will be seen in Figs 2a & b that all contours have to blend with the existing fixed hinge anchoring the downstream end of each flexible liner. The consequence of this is a pronounced increase in working section area with distance downstream of x/B = 0.2. The further consequence is that the Mach number decreases with axial distance in this region, as shown in Ref. 15. The implications of this for testing both half and complete models are discussed in Section 5.

No attempt was made to adapt the walls to compensate for wall-induced upwash. This was done because the tests to be described were made at modest lift coefficients; furthermore, since model lift was measured it was possible to determine the

correction for wall-induced upwash with some confidence (see below).

4 Corrections for wall interference

4.1 Blockage

For all the tests to be described, the standard procedure for allowing for wall interference was used to correct the data. Blockage was determined using linear potential-flow theory in combination with measurements of static pressures at the roof and floor liners [16], [17]. The theory was used to determine a ratio (denoted by λ) at the blockage increment in Mach number at the model to the mean value of the Mach-number increment at four wall stations, two each on the roof and floor. For this purpose, the model was represented by an axial distribution of sources, with corresponding sets of images beyond the test section to represent straight walls. When used with the corresponding pressure measurements made with the model in the tunnel, relative to those in the empty test section with the Mach 1 liner, this method gives a correction to Mach number to allow for model blockage. Corresponding corrections are applied to the free-stream dynamic and (where necessary) static pressures.

Results for the correction to Mach number applied by the standard method to the data for the half model are given in Ref 15. As with the half model, the standard corrections to Mach number for the complete model in the test section with Contour D are only slightly higher than those for the straight walls.

Experience with the standard method [18], suggests that it is tolerant to departures from the assumed straight-wall boundary conditions, for example due to the interaction between the model and the wall boundary layer. It is reasonable, therefore, to expect that the method will show similar tolerance to changes in wall shape. However, small but significant further corrections are expected to be necessary for Mach numbers above 0.85.

Estimates of further corrections to allow for the effect of the wall boundary layers and the change in wall shape have been made using the method described in the Appendix. It is shown there that the additional correction to the blockage increment in streamwise velocity may be expressed as:

$$\delta u_B = (\delta u_B)_{bl} + (\delta u_B)_{fw},$$

where suffixes bl and fw refer to the wall boundary-layer effects and fw to changes in shape of the flexible walls. In addition,

$$(\delta u_B)_{bl} = \lambda_{bl} u_w$$

and

$$(\delta u_B)_{fw} = \Delta u_B - \lambda \Delta u_w$$

are, respectively, the additional corrections due to the a) the influence of the wall boundary-layer/model interaction effects on the λ factor [18] in the straight-wall tunnel and b) change in wall shape. The term u_w is the mean of the measured streamwise velocity increments at corresponding points on the roof and floor of the test section due to the presence of the model, and the symbol Δ denotes increment due to the change from straight to contoured walls.

The results obtained for the half model are illustrated in Figs 3a & b. The additional correction to Mach number due to the wall boundary layer effect, a), is shown in Fig 3a, indicating that the largest correction is obtained with Contour A at M = 0.95. The corrections for the straight walls and Contour A are close to one another. Furthermore, the lowest correction is obtained with Contour B, with the correction for Contour C being roughly midway between those for the other two shaped walls. The reason that B has the smallest correction is that this contour gives the lowest wall Mach number increments of the various wall shapes, and, consequently, the effects of any changes in the λ factor are relatively small.

The effect of wall shaping, b) above, is shown in Fig 3b, which supersedes Fig 13 in Ref. 15 because the new corrections allow for viscous effects where previously they did not. Allowance for wall boundary layers increases the magnitude of the correction for wall shaping, which is at first surprising, and reasons for this are given in the Appendix.

Although the combined corrections are significant and would need to be applied for performance assessment, they do not differ much from one wall contour to another. Thus comparisons between data for the various wall configurations corrected by the standard procedure

to be presented below are only affected by these further corrections in a small way.

Figs 4a and b show the additional corrections for the complete model. The effect of the wall boundary layers on the factor λ (Fig 4a) is virtually independent of the shape change and is small enough to be ignored for Mach numbers below about 0.85. The influence of wall shape change is significant but varies slowly with Mach number (Fig 4b)*.

4.2 Wall-induced upwash

Allowance for the change in angle of incidence due to wall-induced upwash is included using the method of Acum [19]. For this purpose the walls were assumed to be as for the Mach 1 configuration. Thus the effect of the change in wall shape was not represented, although this is expected to be insignificant. Furthermore no allowance was made for the interaction between the wall boundary layers and the lifting effect of the models. It is expected from previous studies [20] that this effect cannot be ignored at high subsonic Mach number. However, as with blockage, it will not significantly affect the comparison between results taken with different wall contours. Finally, the method makes use of the measurement of lift on the model to define the bound and trailing vorticity and so, as with the determination of blockage, use is made of measured flow conditions to represent the effect of the model.

5 Results and discussion

5.1 Combat aircraft half model

A useful indication as to how well the adaptation performs and how reliable the standard correction procedure is can be obtained by comparing wing pressure distributions for the various wall configurations. To illustrate the importance of the correction procedure, results are shown that illustrate the effectiveness of the corrections for blockage. Wing pressure distributions, in p/H form, are shown for the spanwise stations ETA = 0.3 and 0.7 for zero lift in Figs 5a & b. Fig 5a shows results where the experiments have been performed for a given value of the reference Mach number, M_R = 0.9. This Mach number is deduced from the static pressure measurement at the reference tapping far upstream of the model. For each wall shape, the corrected Mach number at the model (determined 'on-line'), M_c, is shown in the captions. The shock position on the wing lower surface differs between the cases, with Contour B, which gives the lowest corrected Mach number, having a shock wave furthest upstream of the four cases. Fig 5b shows pressure distributions that have been obtained at a fixed value of approximately 0.9 for the Mach number corrected by the standard method, 'on-line'. Here there is a very satisfactory collapse of the data, showing that the standard correction procedure provides a satisfactory basis for correcting the data for blockage. After applying the further corrections for wall boundary layer and shaping effects derived from Figs 3a and b, the values of the corrected Mach numbers range from 0.898 for the Mach 1 liners to 0.903 for Contour A.

Corresponding pressure distributions are shown in Figs 6a & b for M_R = 0.928 (Fig 6a) and M_c = 0.95 (Fig 6b). In these cases data for the Mach 1 liners could not be obtained because of choking, and so the comparison is restricted to the three contoured-wall cases. As before, the values of the (fully) corrected Mach number corresponding to the various contours are shown in the caption in Fig 6a. The positions of the lower-surface shock wave are consistent with the corrected Mach numbers, with Contour A, for which the corrected Mach number is the largest of the three cases, having the most downstream shock wave of the three cases. Revision of the corrected Mach number in Fig 6b to allow for the further corrections discussed above gives values of 0.946 ±0.001.

Fig. 7 shows curves of corrected lift, pitching moment and drag coefficient against angle of incidence at where the Mach number corrected by the standard method is held constant at 0.95 for the three contours A, B and C. The lift curves cannot be distinguished to plotting accuracy. However, there are small but significant differences between the results for pitching moment and drag coefficients of Contour B and those for the other two contours. However, this can be explained by the fact that the corrected Mach number for Contour B is slightly lower than the mean value given above. With the refinements to the correction procedure discussed above it should be possible to

* Subsequent to the experiments being performed, it was realised that smaller corrections for wall shaping than those found would have been obtained if the wall static pressure holes used in the determination of Mach number had been placed further downstream.

set the required corrected Mach number to an accuracy of within ±0.001 in the DERA 8ft HST.
In Ref. 15 it is noted that the drag is influenced by the buoyancy arising from the divergence of the walls towards the rear of the test section. While such an effect is obviously of concern for some types of testing, it is not of such importance for half models. Here the concern is rather more with increments (e.g. due to changes in wing section) rather than with absolute values.

5.2 Transport aircraft complete model

Pressure coefficient distributions at a typical outer-wing station, corrected 'on-line' by the standard procedure are shown in Figs 8a and b, respectively for a nominal corrected Mach number of 0.85 and 0.88 and for angles of incidence corresponding approximately to a lift coefficient of 0.5. The agreement between the results for the three wall shapes, Mach 1, D and E is seen to be less satisfactory for $M_c \approx 0.85$ than for $M \approx 0.88$. The explanation for this is that, for this particular wing, the streamwise position of the shock wave is more sensitive to Mach number at $M_c = 0.85$, where the shock wave is in the early stages of formation, than at $M_c = 0.88$. The values of the fully corrected Mach numbers are shown in the captions. For the case $M_c \approx 0.85$, Contour D has a corrected Mach number that is 0.003 lower than that for the straight walls. A plot of shock position against Mach number (not presented) shows that this difference is entirely consistent with the shock wave for Contour D being about 2% chord further upstream than that for the straight walls at $M_c \approx 0.85$. The plot also confirms the relative insensitivity of shock position to Mach number at Mach numbers in the region of 0.88.

Figs 9a and b show corresponding plots of the lift curves, revealing that there is good correlation between the data for the various wall configurations. For commercial reasons drag polars are not presented. It may be noted, however, that the minimum drag coefficient of the model with Contour D is respectively 0.0006 and 0.0007 lower than that with the straight walls at $M_c = 0.85$ and 0.88. The corresponding values for Contour E are 0 and 0.0003 lower than the straight-wall values. These differences can largely be explained by calculated differences in buoyancy drag between the various wall shapes. The divergence of the test section area over the rear of the model (Fig 2b) for Contours D and E causes increasing positive pressure towards the rear of the model, resulting in a reduced drag. The possibility of eliminating this effect by the use of suitable inserts has been considered.

6 Concluding remarks

An assessment of the use of the 8ft High Speed Tunnel to perform tests at high subsonic speeds using adaptive wall technology has been described. The results obtained have shown that the idea of adapting the test section walls is worthwhile, and indicate that, with further effort, this solid-wall wind tunnel could routinely be used for testing at Mach numbers in the region of 0.9 to 0.95. The standard method for correcting Mach number 'on-line' to allow for blockage is shown to yield reasonable correlation between data taken on both a large half model and a sting mounted complete model with quite different wall shapes. Further work is therefore justified to improve this correction method to allow for the small effects due to wall boundary layers and wall shaping.

References

[1] Becker J V. "The high speed frontier: case histories of four NACA programs, 1920-1950", NASA SP-445, 1980.

[2] Bailey A and Wood S A. "The development of a high speed induced wind tunnel of rectangular cross section", ARC R&M 1791, February 1937.

[3] Hornung H G (ed.). "Adaptive wall wind tunnels: technology and applications", AGARD-AR-269, April 1990.

[4] Wedemeyer E, Taylor N J and Holst H. "Adaptive wall techniques", Chapter 10 in AGARD-AG-336, "Wind tunnel wall corrections", Oct 1998.

[5] Ashill P R and Weeks D J. "A method for determining wall interference corrections in solid-wall tunnels form measurements of static pressures at walls.", Paper 1, AGARD-CP-335, 1982.

[6] Ashill P R and Keating R F A. "Calculation of tunnel wall interference from wall pressure measurements.", The Aeronautical Journal, Vol. 92, No. 911, pp 36-53, 1988.

[7] Lewis M C and Goodyer M J. "Two-dimensional wall adaptation for three-dimensional flows", Paper A2 presented at the International Conference on Adaptive Wall Wind Tunnel Research and Wall Interference Correction, Xian, P.R. China, 10-14 June 1991.

[8] Lewis M C, Taylor N J and Goodyer M J. "Adaptive wall technology for three-dimensional models at high subsonic speeds and aerofoil testing through the speed of sound", Paper 42 presented at

the RAeS Conference on Wind Tunnels and Wind Tunnel Testing Techniques, Southampton, UK, 14-17 September 1992.

[9] Ashill P R, Goodyer M J and Lewis MC. "An experimental investigation into the rationale of the application of wind tunnel wall corrections", ICAS 96-3.4.1, September 1996.

[10] Isaacs D. "Calibration of the RAE Bedford 8ft × 8ft wind tunnel at subsonic speeds, including a discussion of the correction to the measured pressure distribution to allow for the direct and blockage effects due to the calibration probe", ARC R&M 2777, 1969.

[11] Cheshire L .J et al. "the design and construction of the compressor for the 8ft × 8ft high speed wind tunnel at RAE Bedford", Proc. Inst. Mech. Eng. vol.172, No.15, 1958.

[12] Barnes T and Dunham C R. "Automatic setting of the flexible walls of a large wind tunnel", Proc. Inst. Elec. Eng. vol.105, Part A, No.21, 1958.

[13] Winter K G. "Methods used in setting the 8ft × 8ft wind tunnel variable supersonic nozzle", RAE TN Aero 2912, 1963.

[14] McKearney P et al. "A variable frequency power installation for large wind tunnel drives", Proc. Inst. Elec. Eng., vol.105, Part A, No.21, 1958.

[15] Taylor, N. J., Ashill, P. R. and Simmons, M. J., "Adaptive wall testing in the DERA 8ft High Speed Wind Tunnel", AIAA 99-0686, Jan. 1999.

[16] Göthert B H. "Transonic wind tunnel testing", AGARD-AG-49, October 1961.

[17] Thom, A., "Blockage corrections in a closed high speed wind tunnel", ARC R&M 2033, November 1943.

[18] Ashill P R, Taylor C R and Simmons M J. "Blockage Interference at High Subsonic Speeds in a Solid Wall Wind Tunnel", Proc. PICAST2/AAC, Vol. 1, Melbourne, 20-23 March 1995.

[19] Acum W E A. "Corrections for symmetrical swept and tapered wings in rectangular wind tunnels", ARC R&M 2948, 1953.

[20] Ashill P R, Jordan R and Simmons M J. "Recent experience in the prediction and assessment of windtunnel wall interference", The Aeronautical Journal, pp 315- 325 Aug. Sept. 1997.

Appendix: Determination of blockage corrections

Let u_w be the mean of the measured streamwise velocity increments at corresponding points on the roof and floor of the test section due to the presence of the model. Then the equivalent streamwise velocity in the straight-wall tunnel is given by:

$$(u_w)_{SW} = u_w - \Delta u_w , \qquad \text{(A1)}$$

where suffixes SW denote straight walls and Δ denotes the increment due to the change from straight to flexible walls.

In the standard technique used for testing with straight walls in the 8ft x 8ft HST the blockage increment in streamwise velocity at the model is determined from the measurements of pressure made at the roof and floor using the simple expression:

$$(u_B)_{SW} = \lambda.(u_w)_{SW} , \qquad \text{(A2)}$$

where λ is a factor deduced from linear theory [16], [17].

The blockage increment in streamwise velocity in the flexible-wall tunnel is given by:

$$\begin{aligned} u_B &= (u_B)_{SW} + \Delta u_B , \\ &= \lambda.(u_w)_{SW} + \Delta u_B \end{aligned} \qquad \text{(A3)}$$

from equation (A2). Equations (A1) and (A3) may be combined to obtain the final expression for the blockage increment in streamwise velocity in the flexible wall tunnel:

$$u_B = \lambda u_w - \lambda \Delta u_w + \Delta u_B . \qquad \text{(A4)}$$

In the standard procedure no allowance is made for the interaction between the model and the wall boundary layers. It is convenient to write

$$\lambda = \lambda_i + \lambda_{bl}$$

where suffixes i and bl respectively refer to inviscid conditions and the effect of the wall boundary layer/model interaction. Thus it is possible to rewrite equation (A4) as:

$$u_B = \lambda_i u_w + \lambda_{bl} u_w - \lambda \Delta u_w + \Delta u_B \qquad \text{(A5)}$$

The first term on the right-hand side is the correction as currently applied. Thus equation (A5) can be written as

$$u_B = \lambda_i u_w + \delta u_B$$

where the additional correction δu_B consists of two parts as follows:

$$(\delta u_B)_{bl} = \lambda_{bl} u_w$$

- due to the effect of the boundary layers on the ratio λ and

$$(\delta u_B)_{fw} = \Delta u_B - \lambda \Delta u_w \qquad \text{(A.6)}$$

due to the change from straight to flexible wall shape. Here suffixes bl refer to the wall boundary layers. Calculations have been made of these effects: for the effect of the wall boundary layers is modelled in the way described in Ref. 18 with one difference. The influence of the wall boundary layers on the inviscid flow in the test section is determined on the assumption that the flow in the test section is one-dimensional. This assumption becomes increasingly accurate as Mach number approaches unity. No allowance is made for interactions between a half model and the boundary layer on the sidewall from which it is mounted. This interaction would normally be considered to an issue associated with the half model technique rather than with wall interference.

Since the wall shaping is uniform across the width of the tunnel it has been possible to treat this effect as a problem in two-dimensional flow. Thus the wall shaping is simulated by line sources (or sinks) and their images beyond the tunnel walls. In these calculations allowance has been made for the effect on the boundary-layer development of the change in wall shape. Here the change in the wall boundary-layer displacement thickness due to the presence of the model is influenced by wall shaping through its effect on wall pressure gradients.

It will be seen in equation (A.6) that the blockage correction for wall shaping depends on two terms. The first, due to the effect of wall shaping on blockage, Δu_B, is smaller in magnitude than the term due to the effect of wall shaping on the wall velocity increment, Δu_w. However, in equation (A.6) the term Δu_w is multiplied buy the factor λ, which is less than unity, the consequence of which is that the first term in the equation Δu_B is the dominant one. Furthermore, the wall boundary layers have the effect of reducing the magnitude of the factor λ, thus increasing the magnitude of the effect of wall shaping on the blockage correction.

Acknowledgement

The authors would like to acknowledge the support of the British Department of Trade and Industry for the study of the transport aircraft complete model.

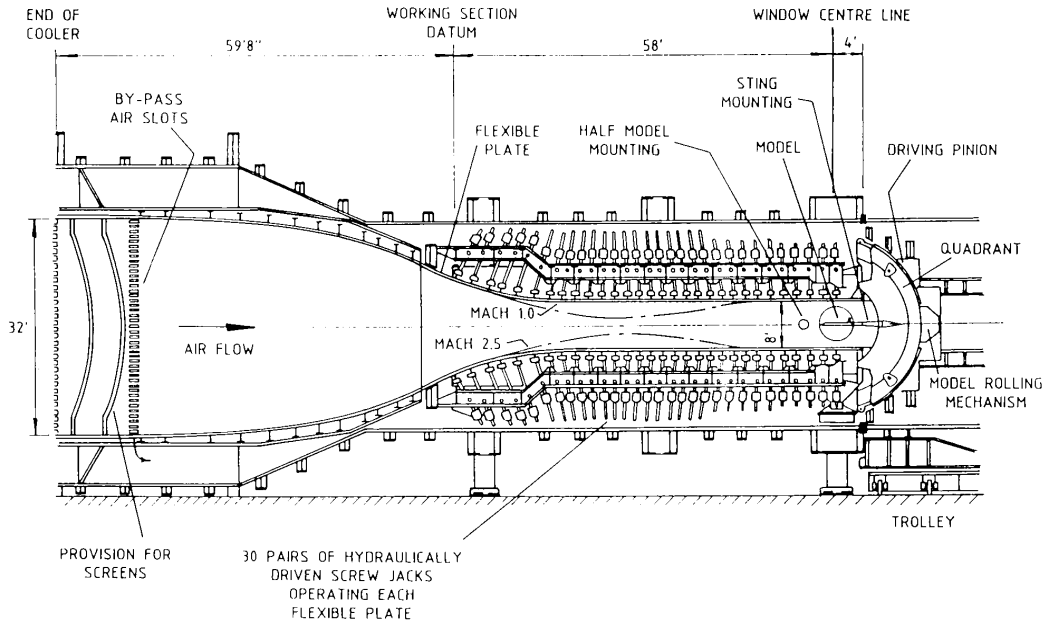

Fig 1 The test section of the DERA High Speed Wind Tunnel (HST)

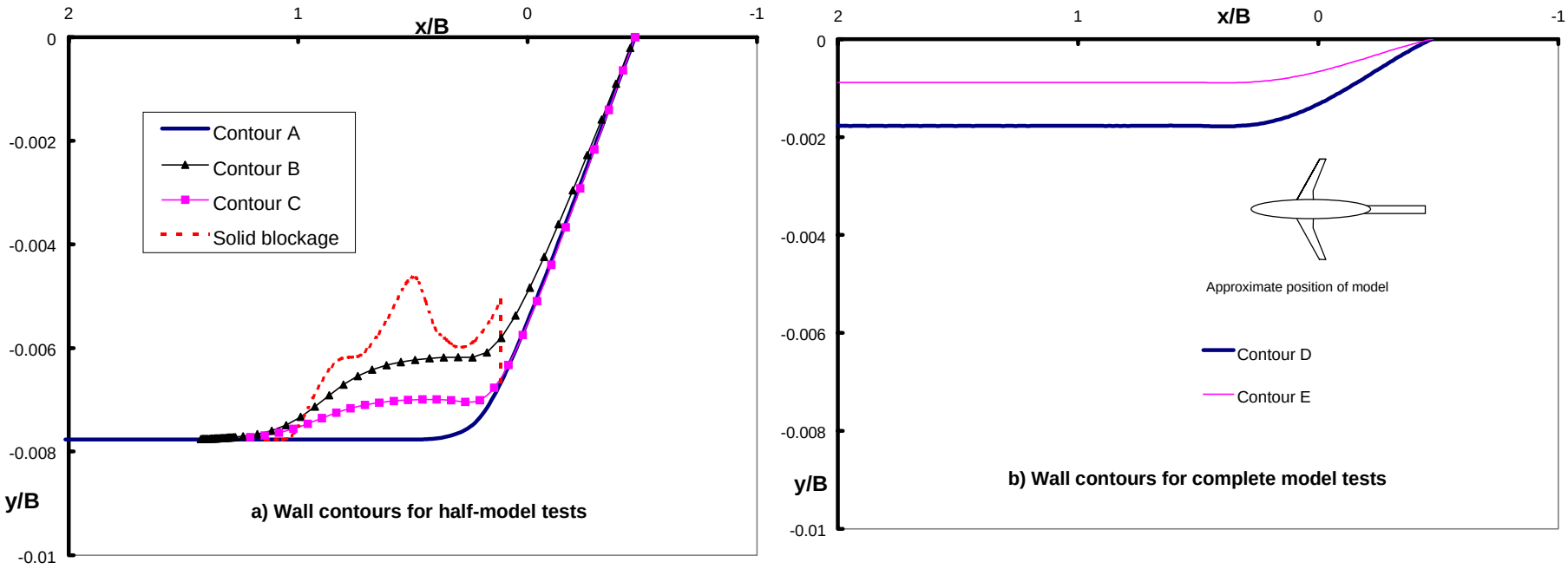

Fig 2 Wall shapes relative to Mach 1 wall shape

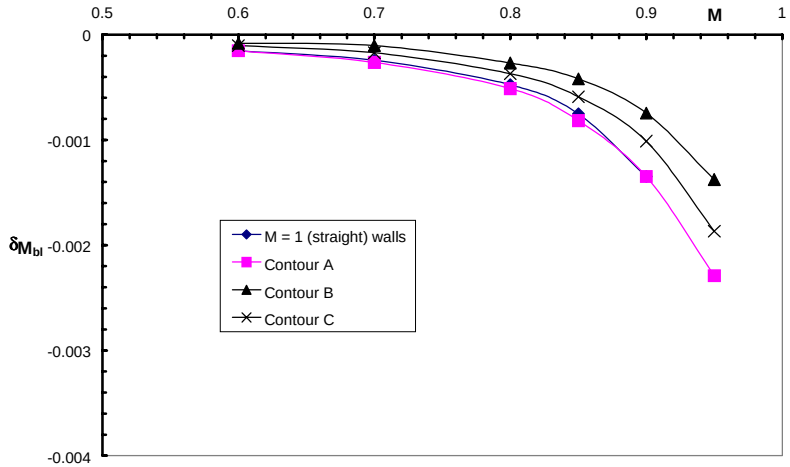

a) Correction to Mach number for the effect of the wall boundary layers on the lambda factor

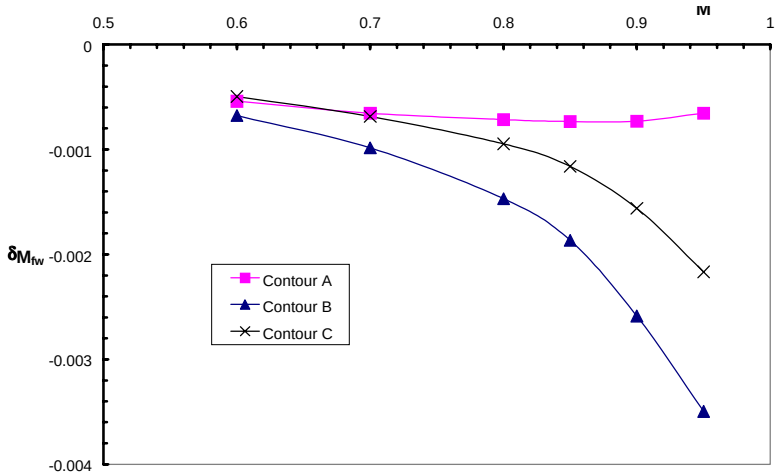

b) Correction to Mach number for wall shape changes

Fig 3 Additional corrections to allow for wall boundary layers and wall shaping (Half-model tests)

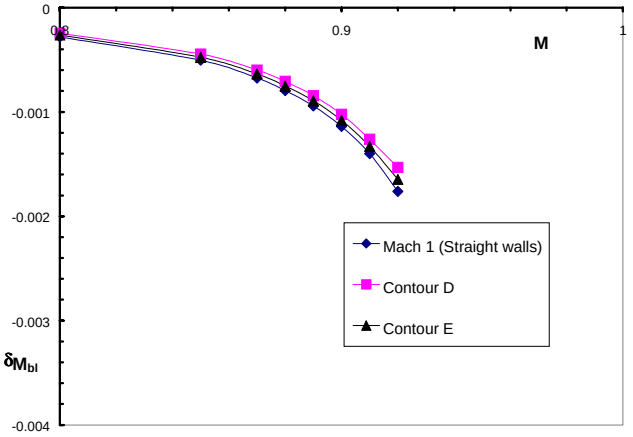

a) Correction to Mach number for the effect of the wall boundary layers on the lambda factor

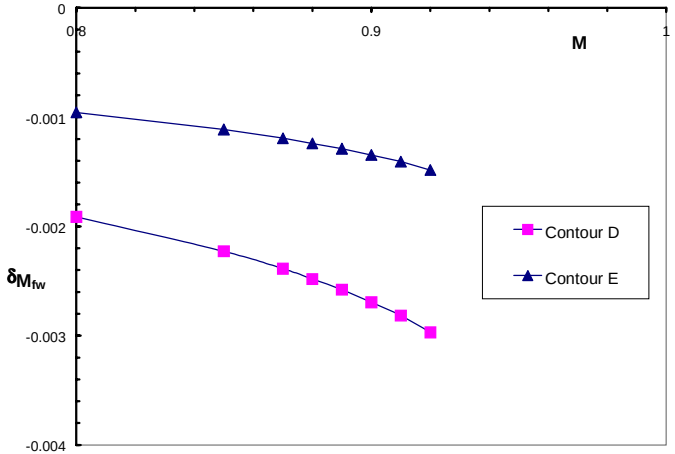

b) Correction to Mach number for wall shape changes

Fig 4 Additional corrections to allow for wall boundary layers and wall shaping (Complete-model tests)

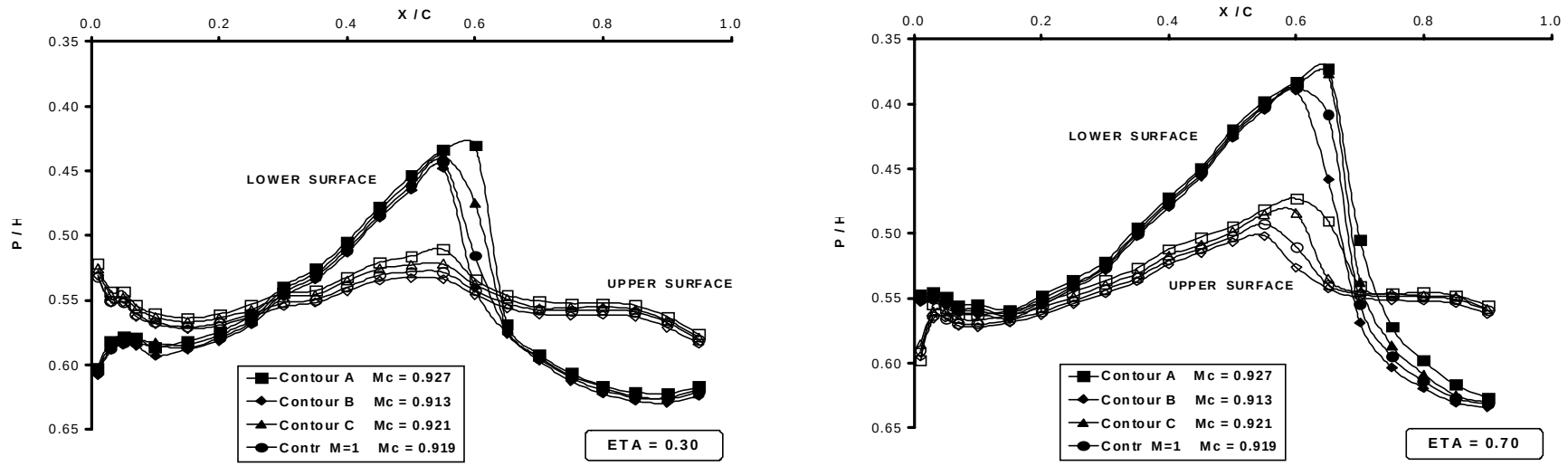

a) Uncorrected Mach number $M_R = 0.90$ $C_L = 0$

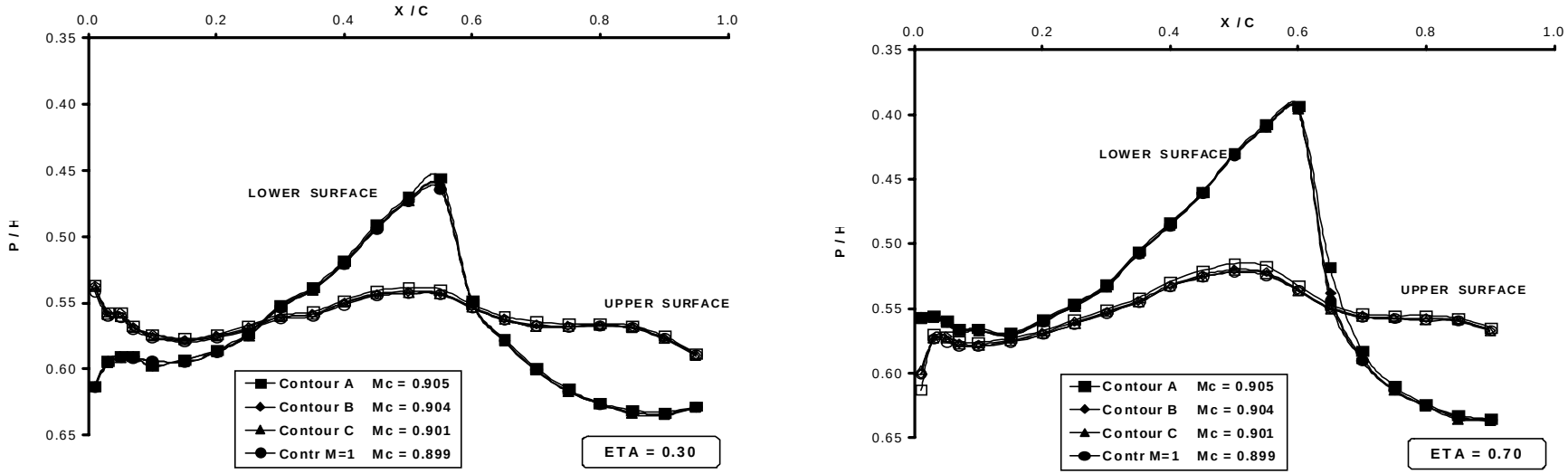

b) Corrected Mach number $M_C = 0.90$ $C_L = 0$

Fig 5 Effect on wing pressure distributions of modifying wall contours

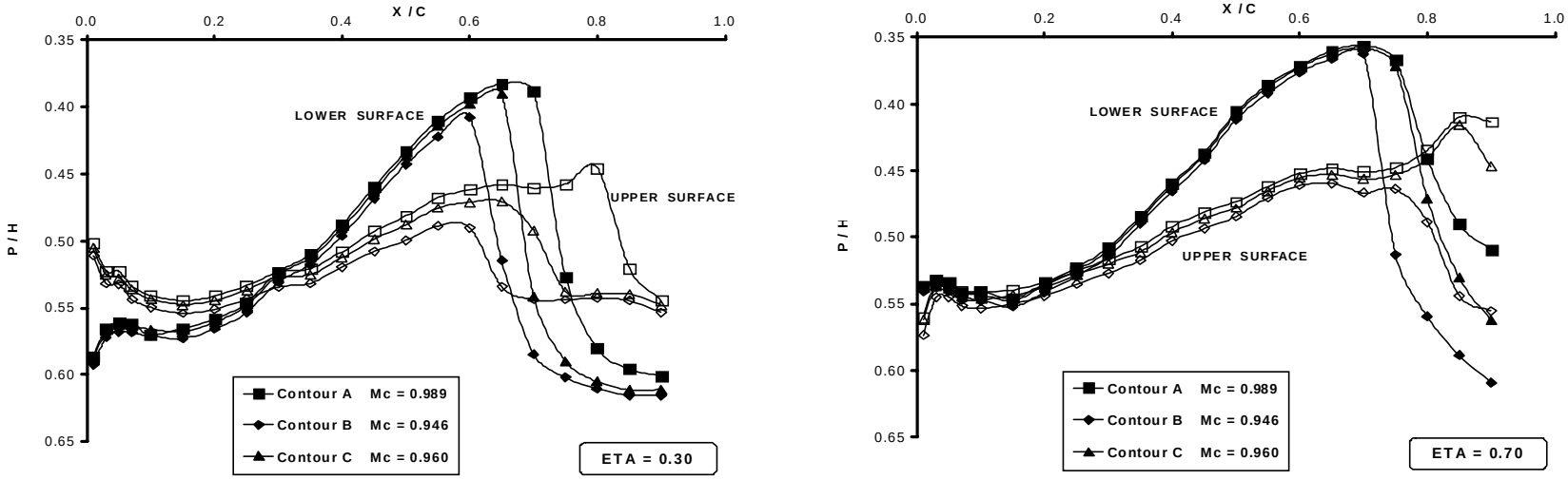

a) Uncorrected Mach number $M_R = 0.93$ $C_L = 0$

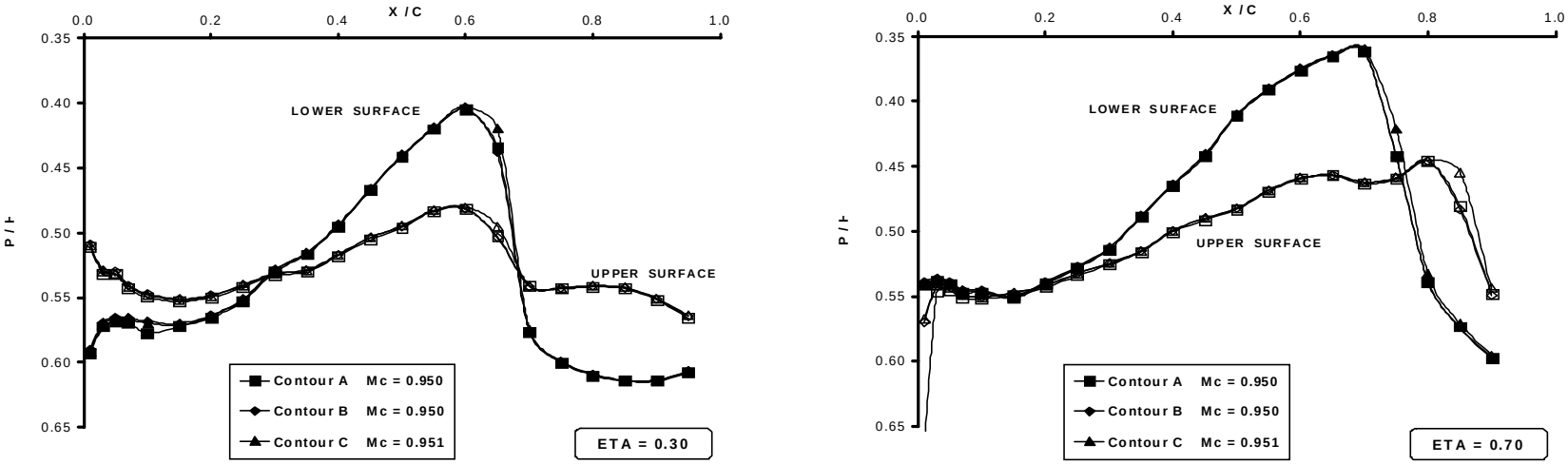

b) Corrected Mach number $M_C = 0.95$ $C_L = 0$

Fig 6 Effect on wing pressure distributions of modifying wall contours

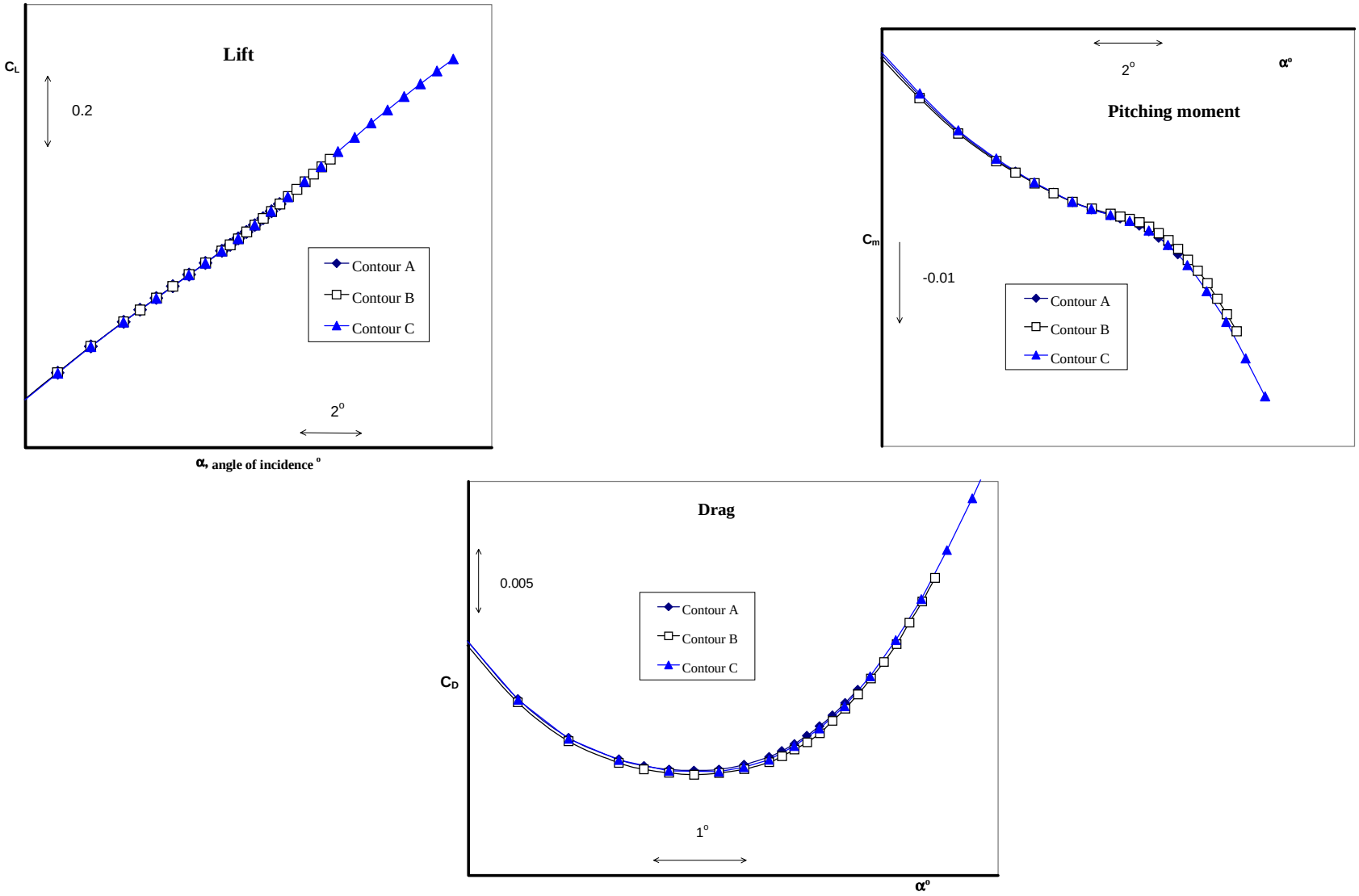

Fig 7 Comparisons of lift, pitching moment and drag – angle of incidence curves, M_c = 0.95

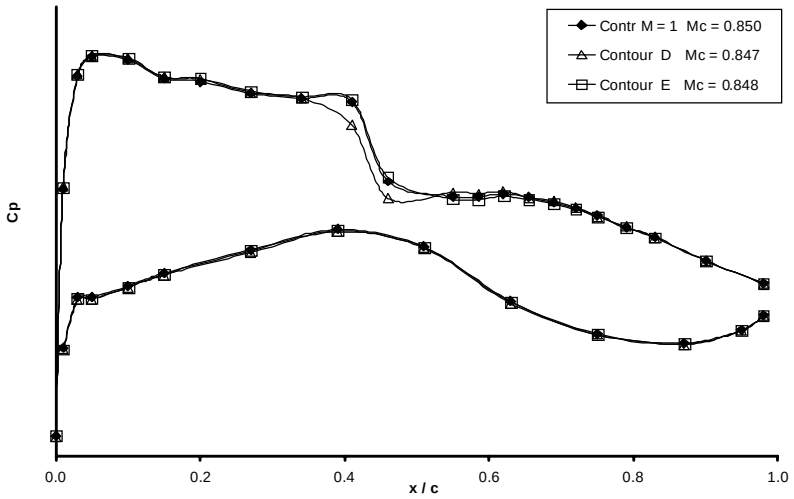

a) $M_C = 0.85$ $C_L = 0.487$

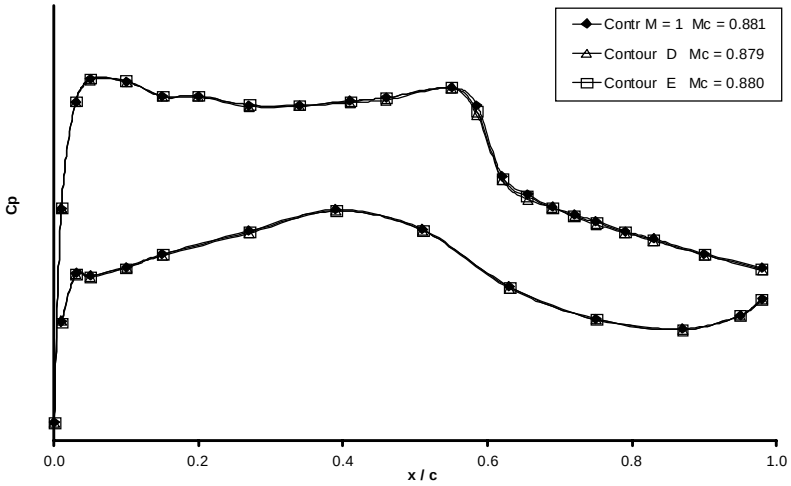

b) $M_C = 0.88$ $C_L = 0.497$

Fig 8 Wing pressure distributions at a typical outer wing station, complete model

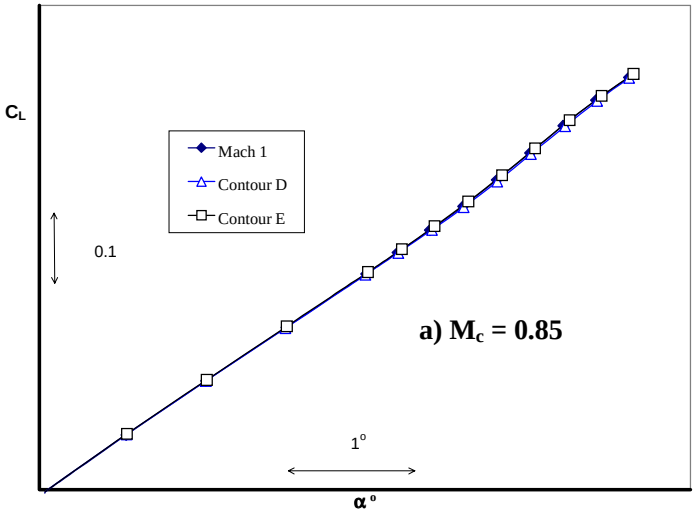

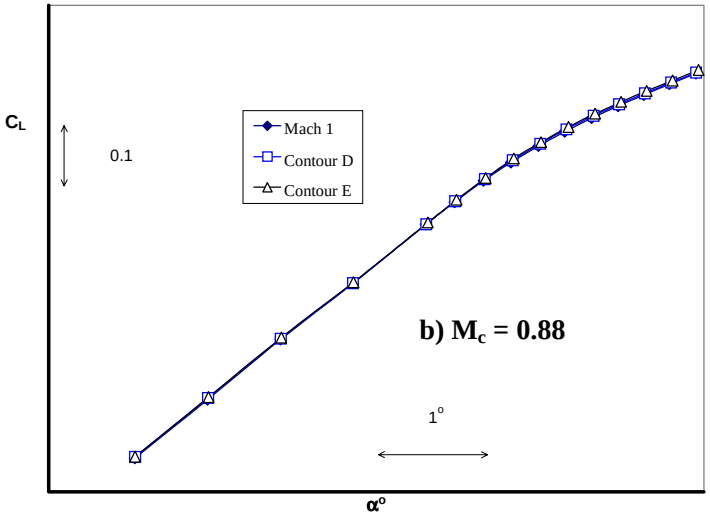

Fig 9 Lift curves, complete model